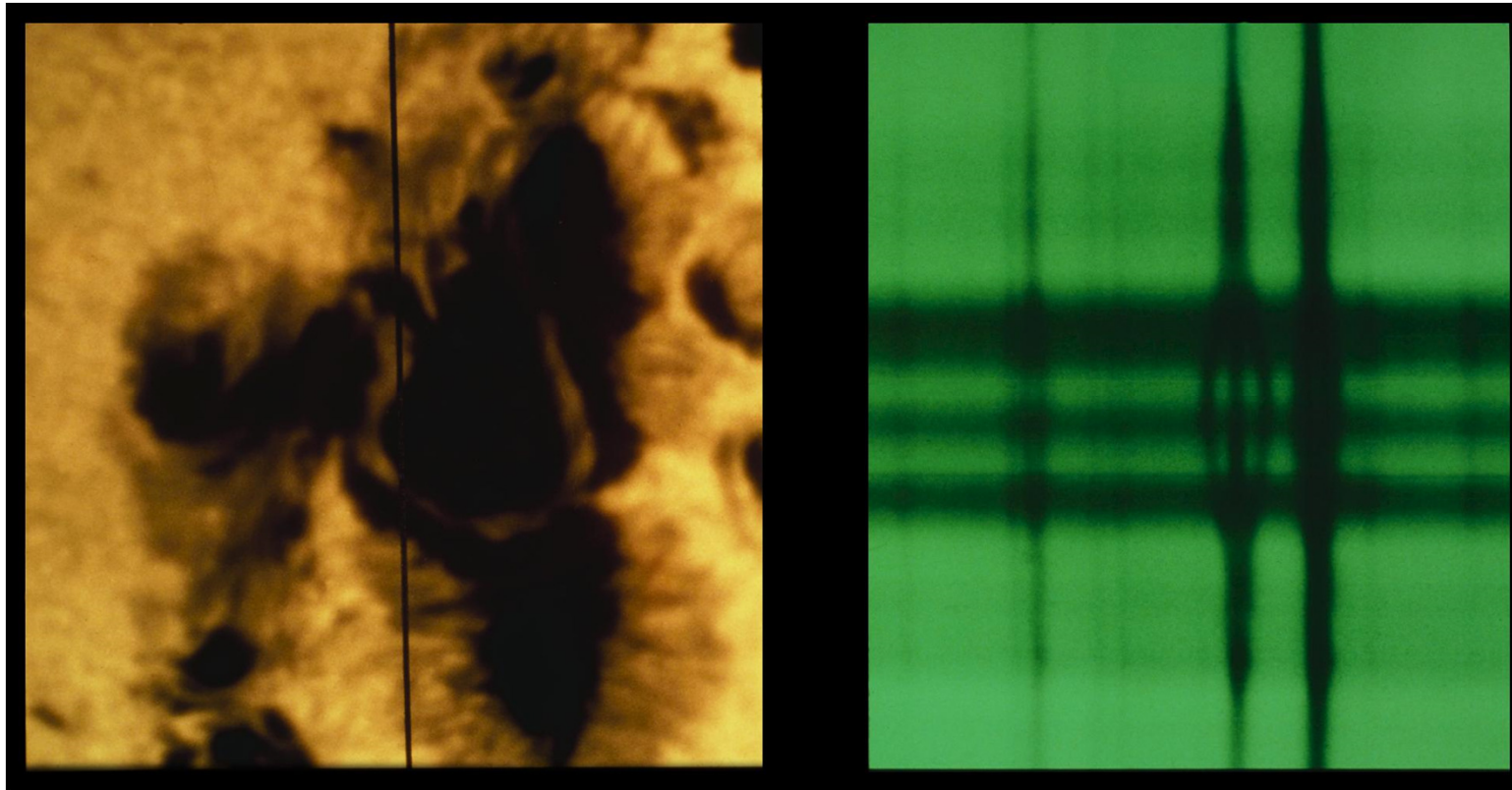


5. Tools for Solar Observations-III

Zeeman effect. Magnetic fields and polarimetry.

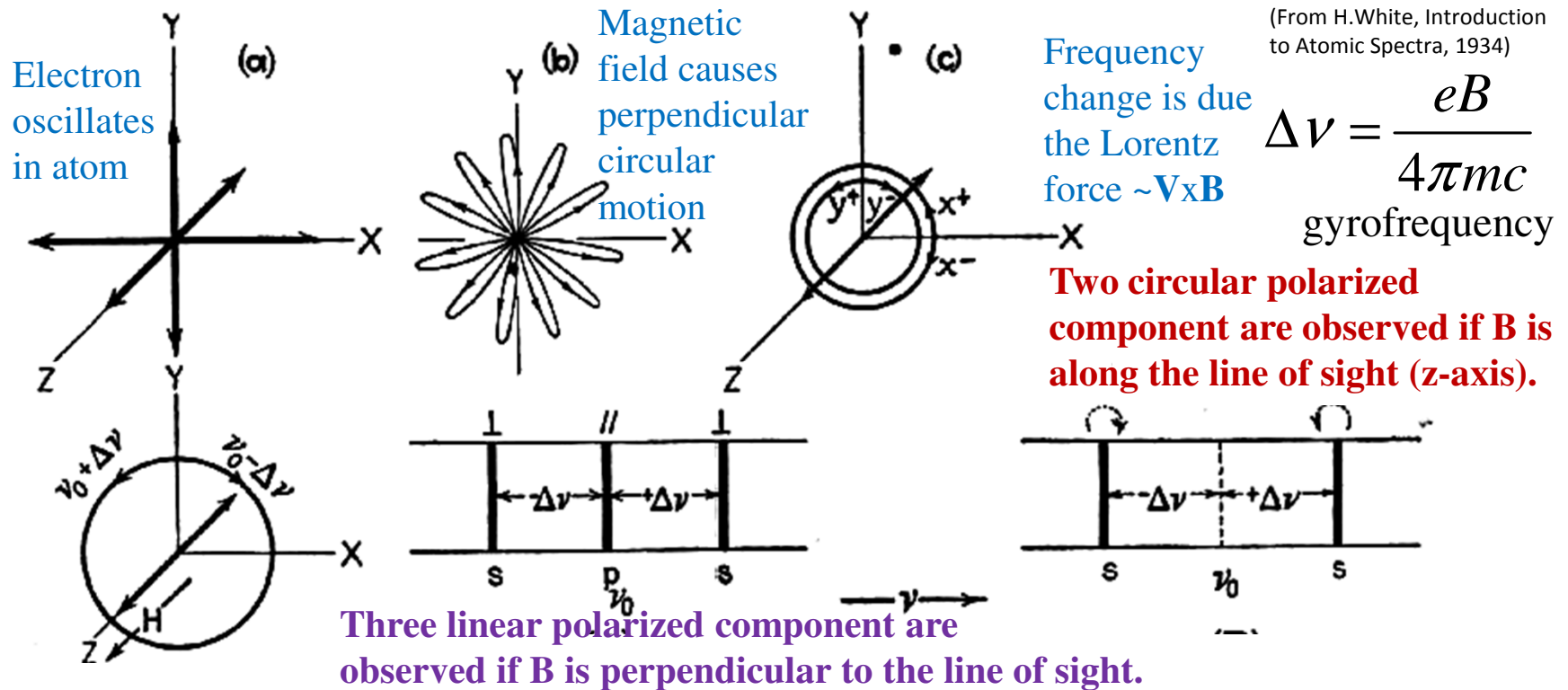
Zeeman effect (observation)

Fe 5250.2A (525nm)



A complex sunspot picture, taken at 15:30 hours UT on 4th July 1974. The vertical black line on the white light image (left) indicates the location of the slit for the spectrograph which took the spectrum, shown on the right. The division of one spectral line into three parts is a clear demonstration of the Zeeman effect. In fact, the Zeeman splitting of this line Fe I at 5250.2A indicates a record field strength of 4130 Gauss. The white light photo shows a sinuous light bridge which divides the spot's umbra into different magnetic polarities. Twenty minutes before this picture was taken, a major white light flare occurred. This picture was taken at the McMath-Pierce Solar Facility on Kitt Peak.

Zeeman effect (classical theory)



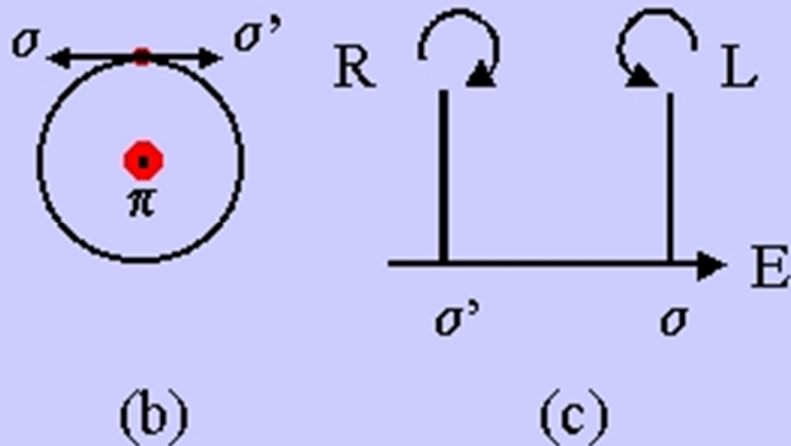
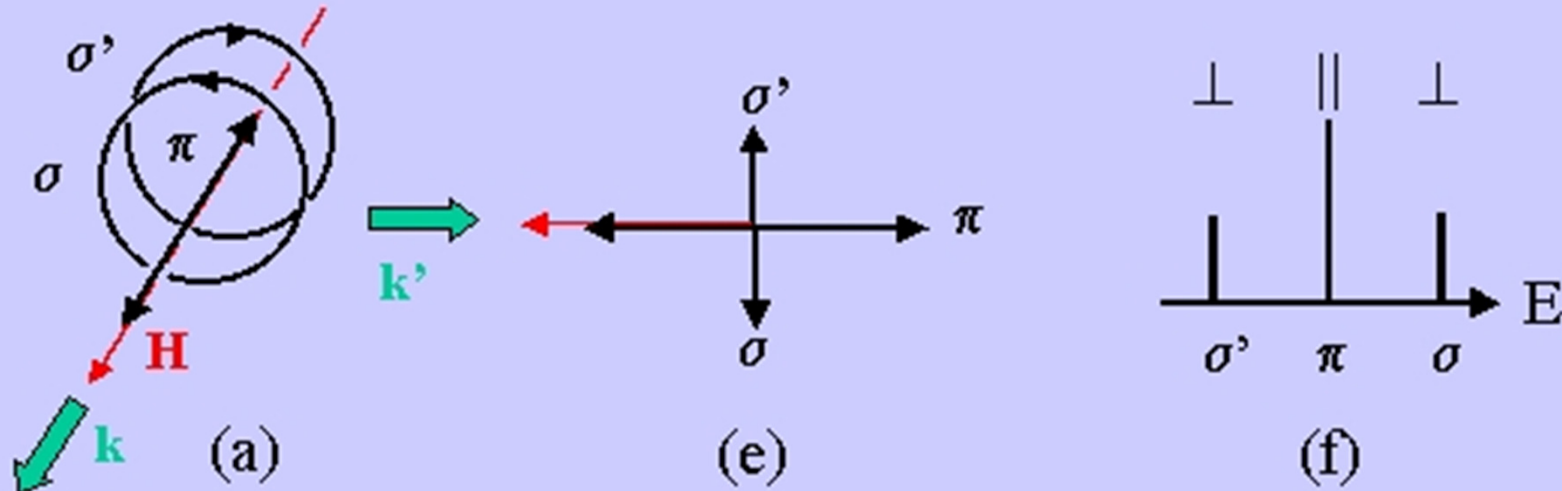
Electrons moving in a counterclockwise direction in the plane of the screen are speeded up by an amount $\Delta\nu$ and those moving in a clockwise direction are slowed down by the same amount. In the absence of a field, the electrons are emitting light. If we observe the radiation in the x direction, only the light from the y and z motions will be observed. Since these motions are projections from all orientations, this light will be *unpolarized*.

In magnetic field, moving transversely to the field, the x and y motions will take the form of rosettes. This motion is equivalent to the resultant of two equal but opposite circular motions as shown in panel c).

When viewed in the direction of the field, only the circular motions are observed, and these produce right- and left-handed circularly polarized light; the z motions will not emit light in the field direction.

When viewed perpendicular to the field, the z motions are observed as plane-polarized light with the electric vector vibrating parallel to the field, and the circular motions, seen edge on, are observed as plane-polarized light with the electric vector at right angles to the field.

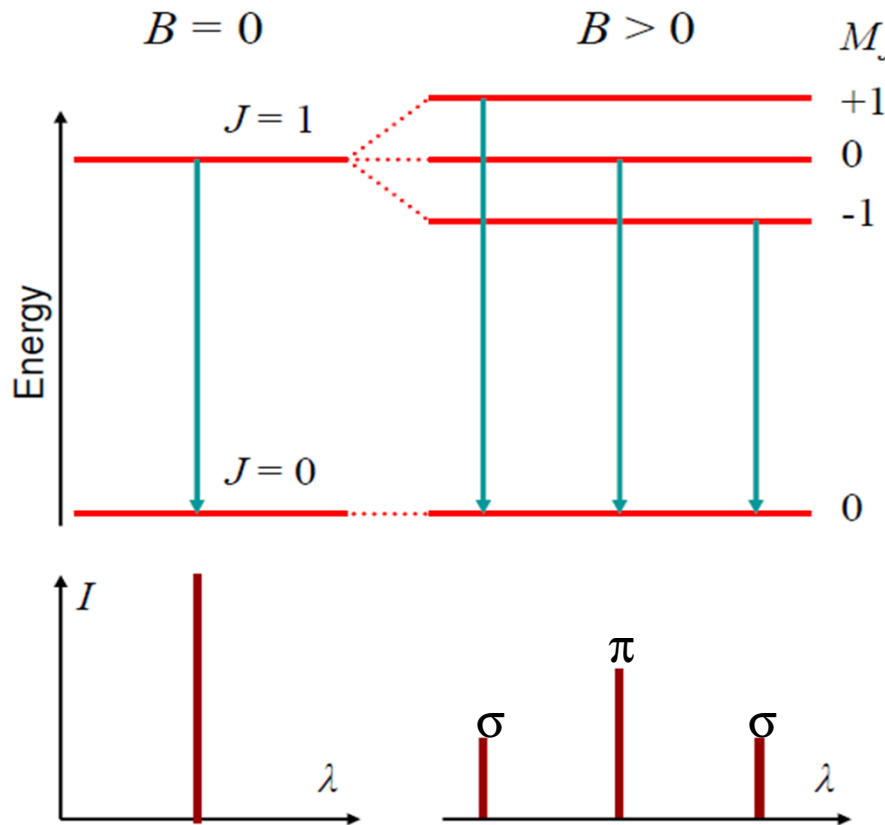
Zeeman and Lorentz (Nobel Prize in Physics, 1902)



When viewed in the direction of the field, only the circular motions are observed, and these produce right- and left-handed circularly polarized light; the z motions will not emit light in the field direction.

When viewed perpendicular to the field, the z motions are observed as plane-polarized light with the electric vector vibrating parallel to the field, and the circular motions, seen edge on, are observed as plane-polarized light with the electric vector at right angles to the field.

Zeeman effect (quantum theory)



M_J Zeeman triplet consists of 2 shifted σ components and one non-shifted π component.

When the line of sight is in the direction of the field (longitudinal Zeeman effect) we see only σ components circularly polarized in opposite sense.

If we look perpendicular to the field we see three components: π is linearly polarized parallel to \vec{B} , and σ components are linearly polarized perpendicular to \vec{B} . There is no information about the direction of vector \vec{B} .

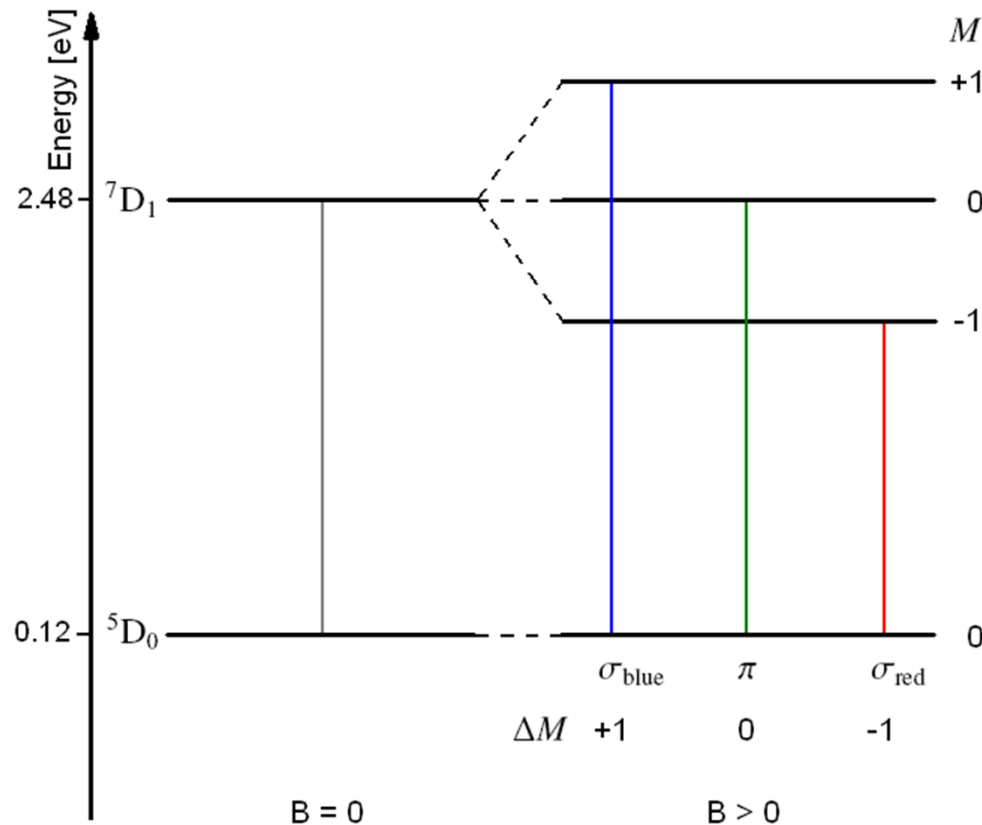
$$\lambda - \lambda_0 = \frac{e}{4\pi cm_e} g^* \lambda^2 B \quad g^* = gM - g' M' \quad \text{g-factor of the transition}$$

$$g = 1 + \frac{J(J+1) + S(S+1) - L(L+1)}{2J(J+1)}$$

Lande factor

- L is the total orbital moment of the electrons
- S is the spin quantum number
- J is the total angular momentum
- M_J is the magnetic quantum number: $-J, \dots, J$

Normal Zeeman splitting for iron line Fe I 525.02 nm



Standard notation $^{2S+1}L_J$ provides information about quantum numbers L , S and J .

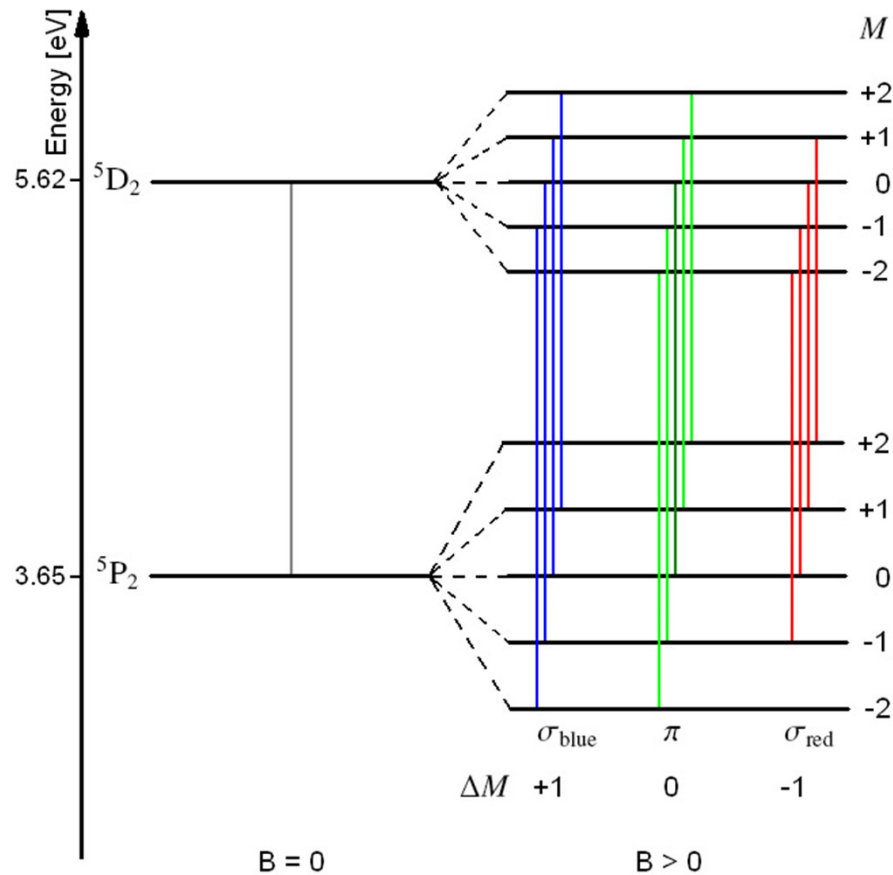
The letters S, P, D, F, \dots mean an orbital angular momentum corresponding to $L=0, 1, 2, 3, \dots$

7D_1 means $L=2, S=3, J=1$.

Zeeman splitting for the iron line at 525.02 nm formed by transition between the energy levels $^5D_0 \leftrightarrow ^7D_1$. Because of $J = 0$, the lower energy level 5D_0 is not degenerate, i.e. it does not split in the presence of a magnetic field. The upper $J = 1$ level splits into three different sublevels with the magnetic quantum numbers $M = -1, 0, +1$.

A Lorentz triplet is formed, which is named the normal Zeeman effect. The formation of exactly three split lines is a particular case that only occurs when one of the two energy levels has $J = 0$.

Anomalous Zeeman splitting for iron line Fe I 630.15nm



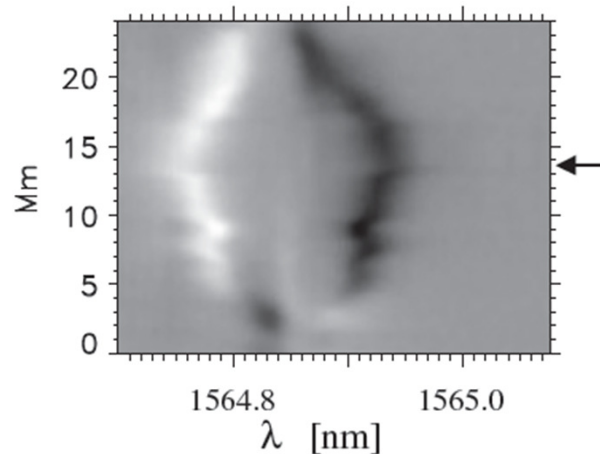
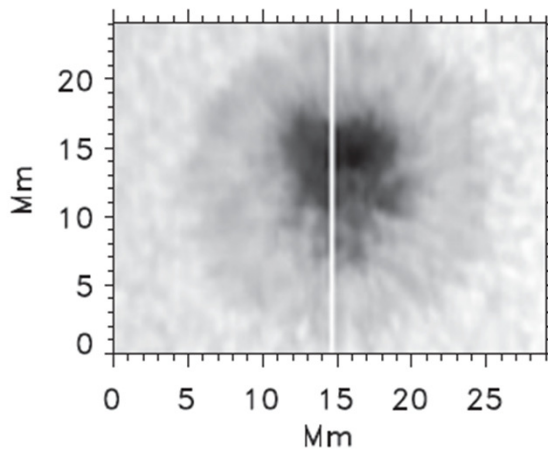
Not all transitions are allowed. The magnetic quantum number m of the two energy levels must not differ by more than one.

In a general (more common) case more than three components are observed (anomalous Zeeman effect). The anomalous Zeeman effect is illustrated for the $5P_2 \leftrightarrow 5D_2$ transition of the iron line at 630.15 nm. Both energy levels have $J = 2$ but the different Landé factors, 1.8333 and 1.5, so that the line splits into 13 components. Effective g -factor (g^*) is prescribed in this case.

Zeeman effect (observation)

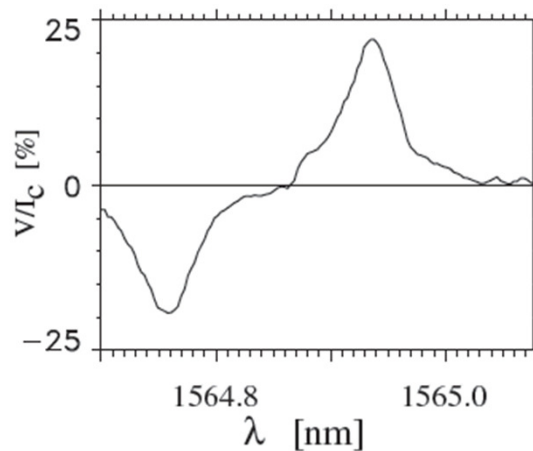
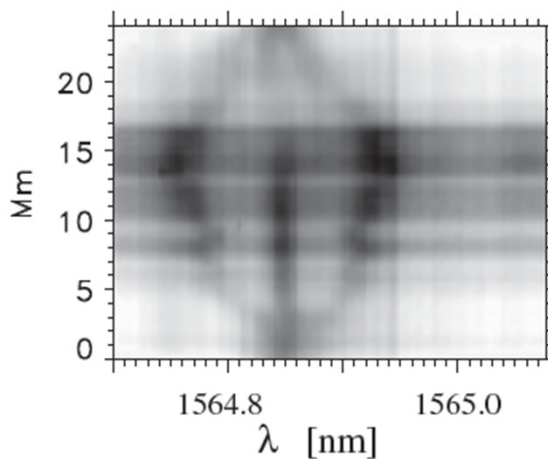
$$\lambda - \lambda_0 = 4.67 \times 10^{-5} g^* \lambda^2 B$$

Numerical formula for the line displacement in cm, B is in Gauss. The Zeeman splitting is higher for longer wavelength and larger g-factor.



Zeeman splitting and circular polarization of the infrared Fe I line at 1564.8 nm ($g=3$).

The white line is the slit position for the spectrum shown in the *lower left*. T



The *upper right* panel shows the circular polarization, with an arrow marking the position of the Stokes $V(\lambda)$ profile in the *lower right*.

Observation was performed on 9 Nov 1999 at the German Vacuum Tower Telescope

Magnetic Field Measurements

Magnetic field causes two effects on spectral properties:

1. frequency shift (Zeeman splitting)
2. polarization

Most magnetic field measurements are based on observation of polarization in absorption lines. Polarization is orientation of electric field vector in EM wave.

Consider EM wave with components:

$$E_x = A_1 e^{i(\phi_1 - \omega t)} \equiv E_x e^{-i\omega t},$$

$$E_y = A_2 e^{i(\phi_2 - \omega t)} \equiv E_y e^{-i\omega t}.$$

If $\phi_1 - \phi_2 = 0$ then the wave has linear polarization. If $\phi_1 - \phi_2 = \pm\pi/2$ then the wave has circular polarization.

Polarization matrix:

$$I_{i,j} = \langle E_i^*(t) E_j(t) \rangle,$$

where $\langle \dots \rangle$ is average over statistical sample.

Polarization matrix: $I_{i,j} = \langle E_i^*(t)E_j(t) \rangle$,

where $\langle \dots \rangle$ is average over statistical sample.

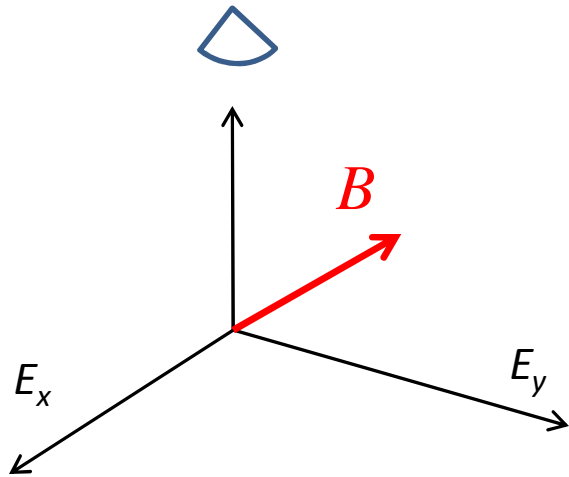
Stokes parameters:

$$I = k(\langle E_x^*E_x \rangle + \langle E_y^*E_y \rangle),$$

$$Q = k(\langle E_x^*E_x \rangle - \langle E_y^*E_y \rangle),$$

$$U = k(\langle E_x^*E_y \rangle + \langle E_y^*E_x \rangle),$$

$$V = k(\langle E_x^*E_y \rangle - \langle E_y^*E_x \rangle).$$



$$\text{Polarization degree } P = \left(\frac{Q^2 + U^2 + V^2}{I^2} \right)^{1/2}$$

The magnetic field measurement procedure consists of three steps:

1. measure $I(\lambda), Q(\lambda), U(\lambda), V(\lambda)$
2. relate $I(\lambda), Q(\lambda), U(\lambda), V(\lambda)$ to \vec{B} using a radiation transfer theory
3. find \vec{B} by solving the inverse problem (“Stokes inversion”)

Description of the state of polarization: the Stokes vector $\{I, Q, U, V\}$

Denote the phase difference between the electric vectors along the x- and y-axes as

$$\delta = E_x - E_y$$

The operational definition of the Stokes parameters are then as follows:

$$I = I_{\leftrightarrow} + I_{\updownarrow} = I_{\nearrow} + I_{\searrow} = \langle E_x^2 \rangle + \langle E_y^2 \rangle$$

$$Q = I_{\leftrightarrow} - I_{\updownarrow} = \langle E_x^2 \rangle - \langle E_y^2 \rangle$$

$$U = I_{\nearrow} - I_{\searrow} = 2\langle E_x E_y \cos \delta \rangle$$

$$V = I_{\odot} - I_{\ominus} = 2\langle E_x E_y \sin \delta \rangle$$

$$I = \text{total intensity} = I_{\text{lin}}(0^\circ) + I_{\text{lin}}(90^\circ)$$

$$Q = I_{\text{lin}}(0^\circ) - I_{\text{lin}}(90^\circ)$$

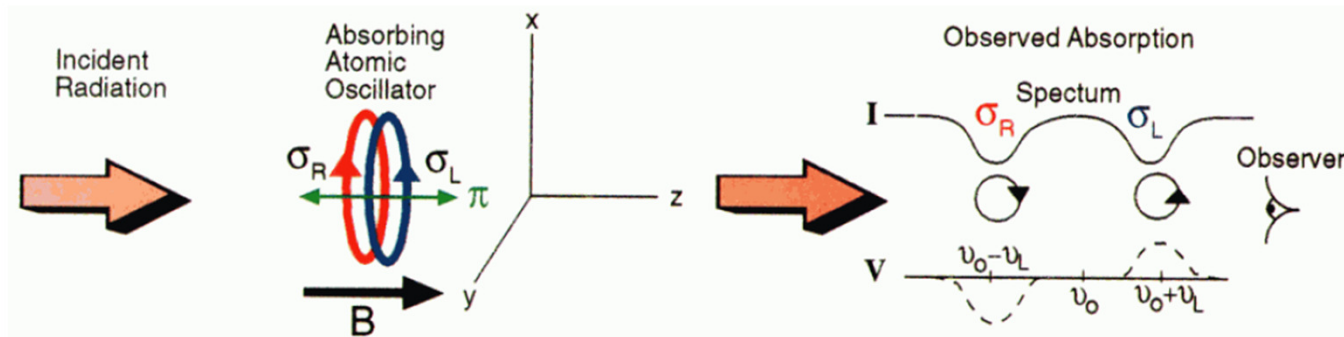
$$U = I_{\text{lin}}(45^\circ) - I_{\text{lin}}(135^\circ)$$

$$V = I_{\text{circ}}(\text{right}) - I_{\text{circ}}(\text{left})$$

Note: Stokes parameters are sums and differences of intensities, i.e. they are directly measurable

Formation of absorption Stokes profiles

Longitudinal Zeeman Effect



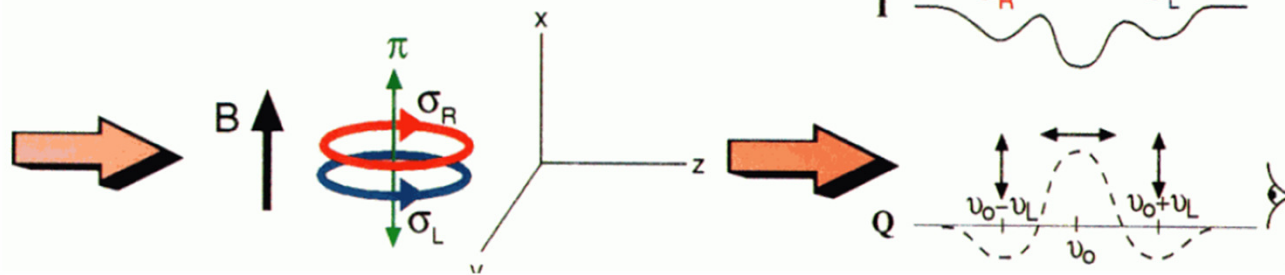
$$I = I_{\leftrightarrow} + I_{\updownarrow}$$

$$Q = I_{\leftrightarrow} - I_{\updownarrow}$$

$$U = I_{\nearrow} - I_{\searrow}$$

$$V = I_{\circlearrowleft} - I_{\circlearrowright}$$

Transverse Zeeman Effect

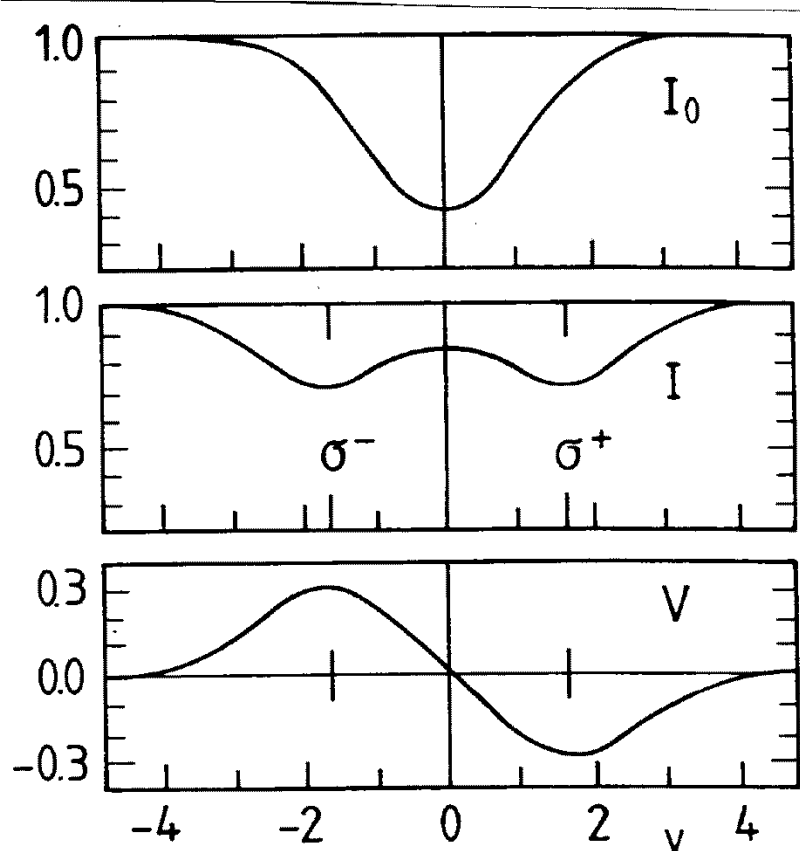


(from B.Lites, 2000)

The longitudinal Zeeman effect occurs when a plane wave propagating in the direction of B excites both circular modes, σ_R and σ_L , corresponding to right- and left circular polarization, respectively, leading to the absorption of circularly polarized light at the shifted frequencies. These circular modes correspond to the σ components of the Zeeman pattern. In this case the light propagates along B , and the incident electromagnetic wave has no oscillatory component along the linear oscillator parallel to B (the π component), so absorption of that component cannot occur. Because the background continuum is unpolarized, the absorption of right- (left) circular polarization results in an excess of left- (right)-circular polarization in the residual intensity as evidenced by negative (positive) Stokes V .

In the **transverse Zeeman effect** the propagating wave excites both σ and π components. π is unshifted, and σ only influences the state of linear polarization of the incident beam that is perpendicular to B , or along y . The three components of the Stokes Q profile (up-down minus left-right linear polarization) are identified with the linear polarizations resulting from the absorption process. The Stokes U is zero in this case because B is oriented along x .

Longitudinal Zeeman effect



Consider Stokes profiles for an absorption line formed in a layer of optical thickness τ illuminated by continuum intensity I_C

$$I = I_C(1 - \tau) - I_C\tau(\eta^+ + \eta^-)/2$$

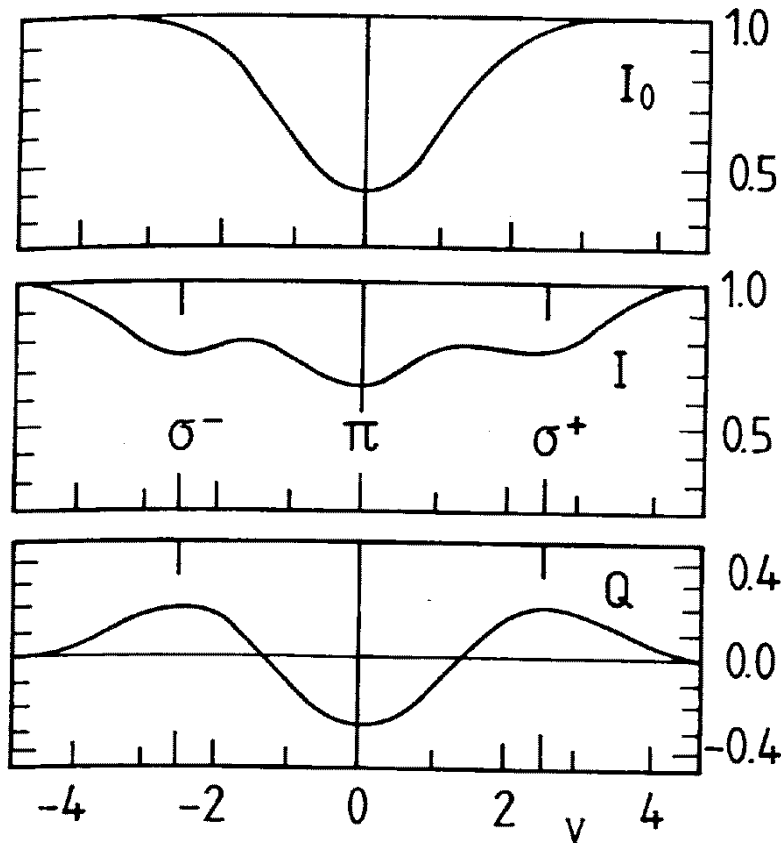
uniform attenuation shifted absorption line profiles.

$$\eta^\pm = \eta(\lambda \pm \Delta\lambda_B)$$

$$V(\lambda) = -I_C\tau(\eta^+ - \eta^-)/2$$

Longitudinal Zeeman effect. Magnetic field has only component along the line of sight. Stokes V-profile is antisymmetrical; Stokes profiles $Q=U=0$.

Transverse Zeeman effect



Consider magnetic field is parallel to axis x . The line of sight is along z axis.

$$I = I_C(1 - \tau) - I_C\tau \left(\frac{1}{2}\eta + \frac{1}{4}(\eta^+ + \eta^-) \right)$$

$$Q = -I_C\tau \left(\frac{1}{2}\eta - \frac{1}{4}(\eta^+ + \eta^-) \right) ,$$

Transversal Zeeman effect. The intensities of the $(\sigma^+, \pi, \sigma^-)$ triplet are in the ratios $1/4:1/2:1/4$ and that the linear polarizations of the σ are π components are perpendicular, and hence contribute with different signs to Q . In this case $U = V = 0$.

Weak-field approximation

In a general case, the absorption line profiles $\eta^\pm = \eta(\lambda \pm \Delta\lambda_B)$ are calculated numerically by solving the radiation transfer equations.

Consider the case when the Zeeman splitting is much less than the Doppler linewidth:

$$\Delta\lambda_B \ll \Delta\lambda_D,$$

where $\Delta\lambda_D = v_T \lambda / c$ the Doppler linewidth due to thermal velocity v_T .

In this case we may consider expansion of function η_\pm in terms of $\Delta\lambda_B$:

$$\eta^\pm \simeq \eta_0 \pm \frac{\partial\eta}{\partial\lambda} \Delta\lambda_B + \frac{\partial^2\eta}{\partial\lambda^2} \frac{\Delta\lambda_B^2}{2}.$$

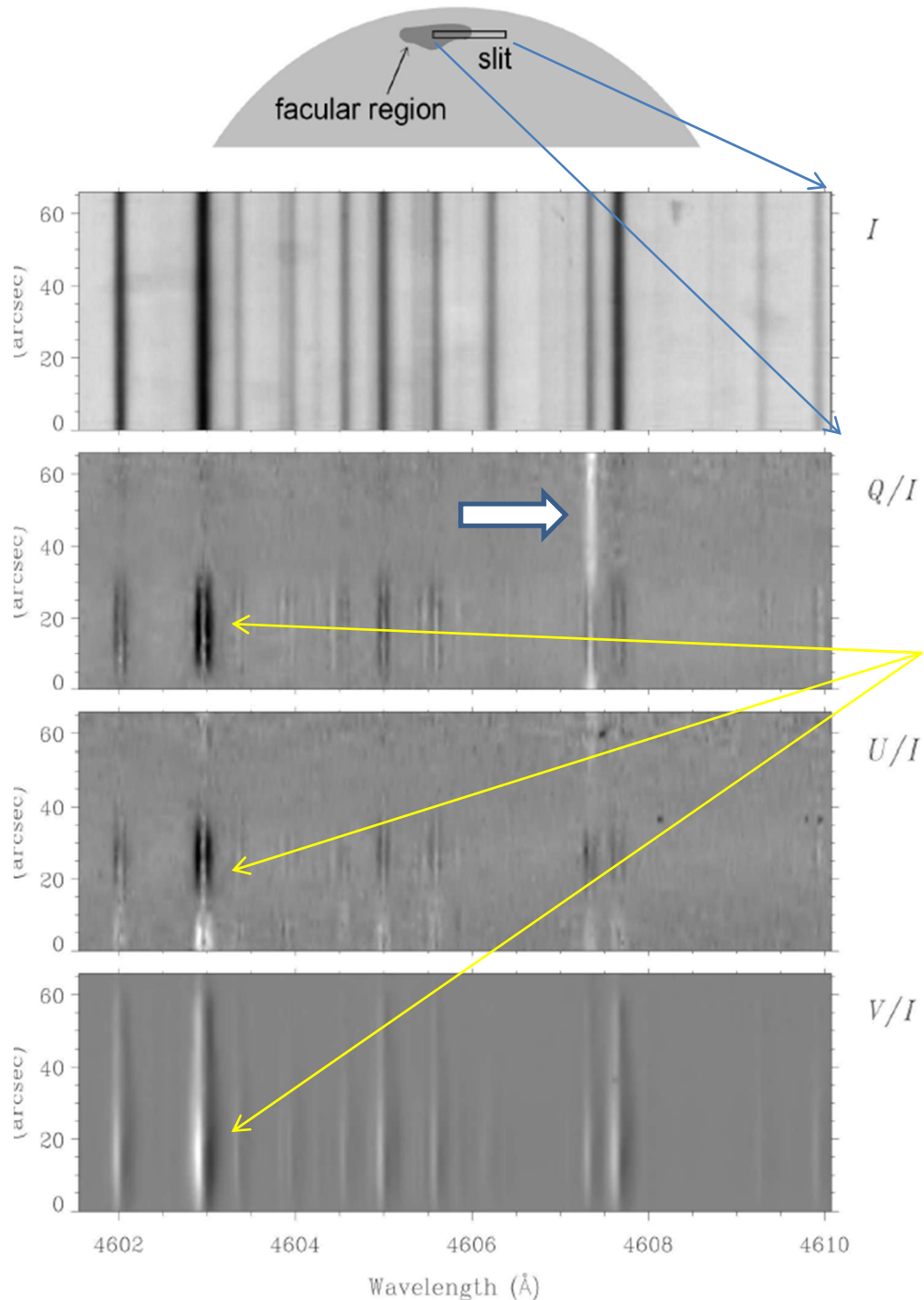
Then, for the longitudinal Zeeman effect:

$$V \propto 2 \frac{\partial\eta}{\partial\lambda} \Delta\lambda_B \propto B,$$

and for the transversal effect:

$$Q \propto \frac{\partial^2\eta}{\partial\lambda^2} \Delta\lambda_B^2 \propto B^2.$$

The transverse effect is quadratic in B, and is much smaller than the longitudinal effect.

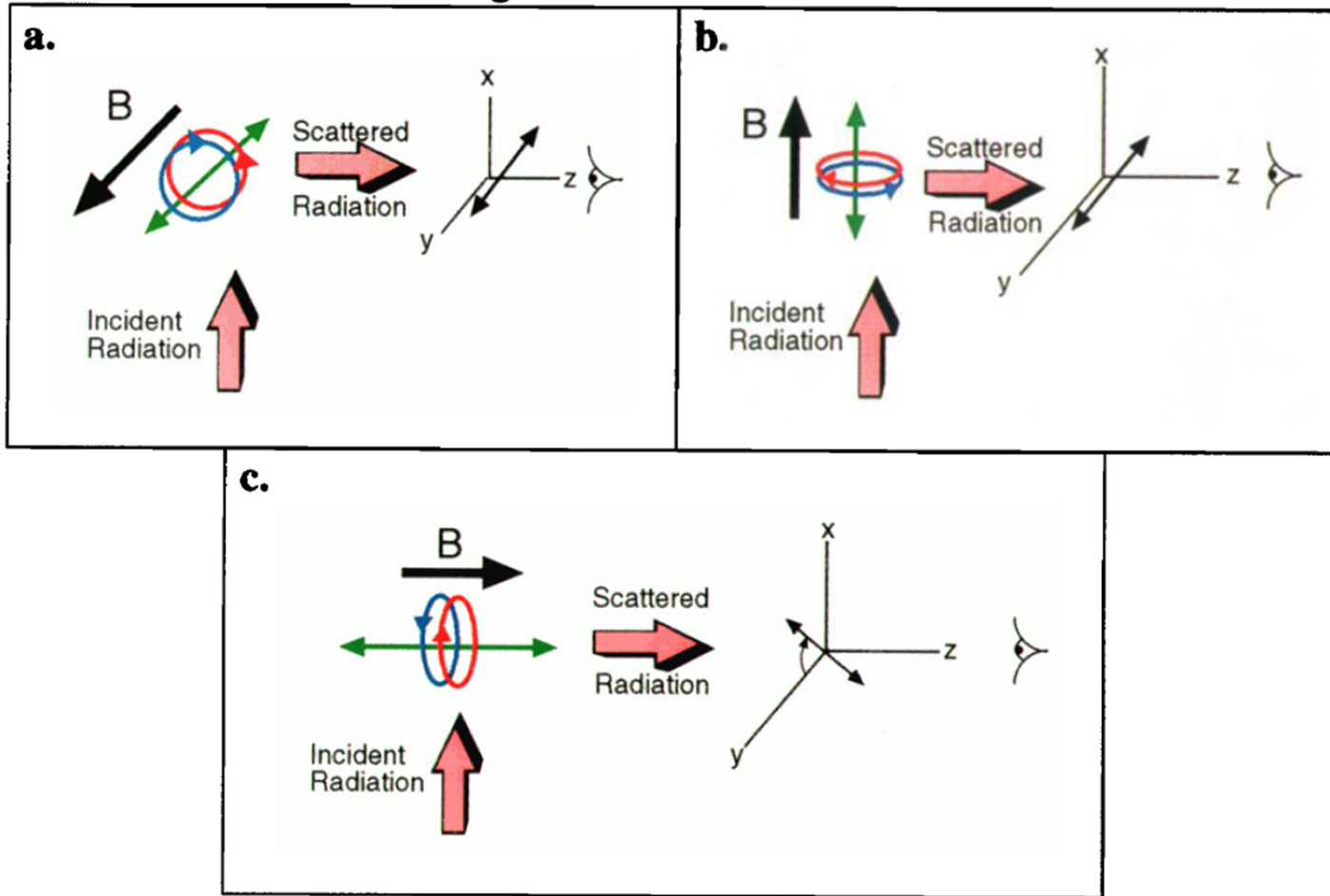


Spectropolarimetric observation close to the edge of the solar disk with half of the spectrograph slit crossing a moderately magnetized facular region.

Note that while the characteristic signature of the longitudinal Zeeman effect is present at all spatial points along the slit, the signature of the transverse Zeeman effect disappears as soon as one goes outside the facular region.

Interestingly, the only spectral line which shows linear polarization outside the facular region is the Sr I (Strontium) line at 4607 \AA with a Q/I shape that has nothing to do with the transverse Zeeman effect. This is due to the **Hanle effect**.

Hanle Effect in Scattering



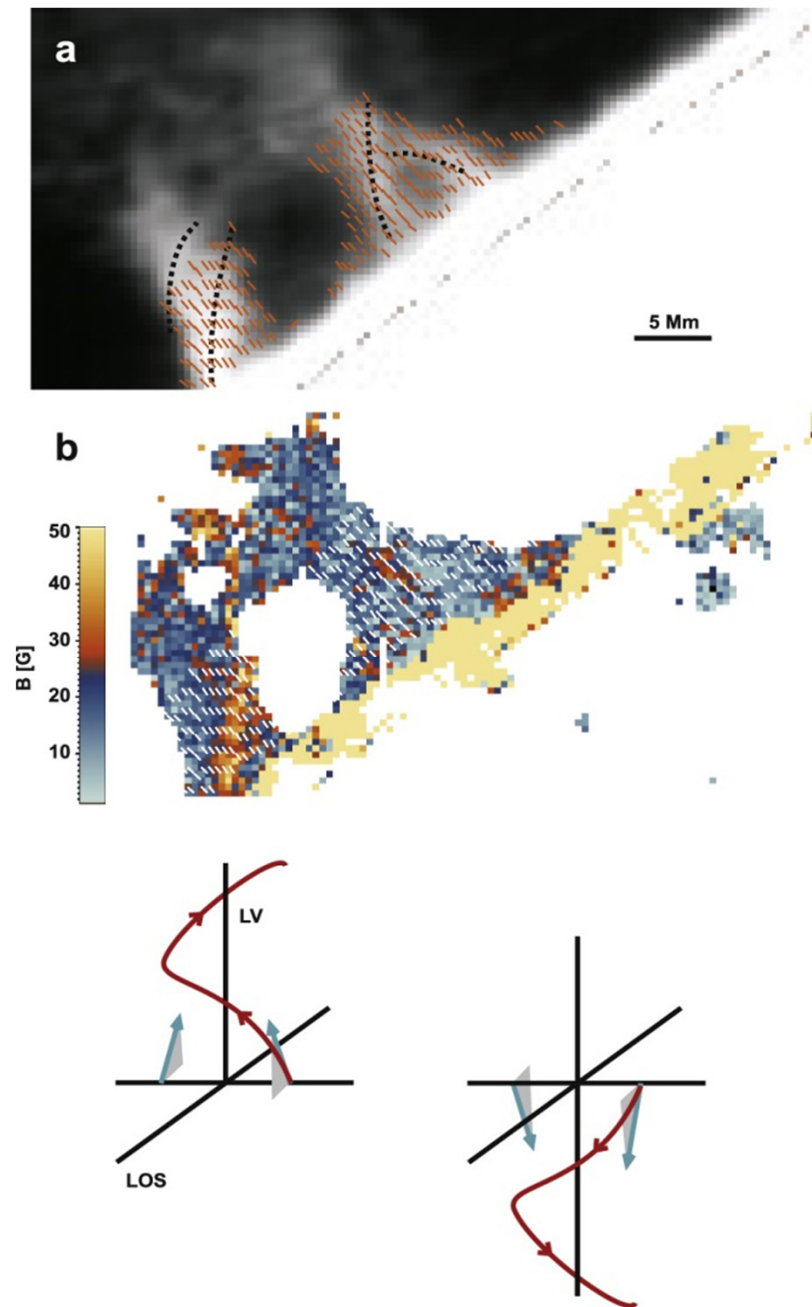
(from Lites, 2002)

A scattering system illuminated anisotropically by a plane wave propagating along the x axis. Assume the magnetic field is directed along the y axis and the observer is positioned along the z axis (panel a). For pure scattering in the absence of a magnetic field the observer would measure pure linear polarization oriented parallel to the y axis: No excitation and reemission of polarization occurs along x because the incident wave has no corresponding component of the electric field. As with the Zeeman effect, we represent the oscillator by a linear oscillator along y and two oppositely rotating circular oscillators in the x - z plane. The magnetic field causes a mixing of the field-aligned state with the circular states, causing some reemission polarized along x . Therefore, in this geometry, the Hanle effect reduces the net polarization of the scattered radiation but does not alter its orientation along the y axis.

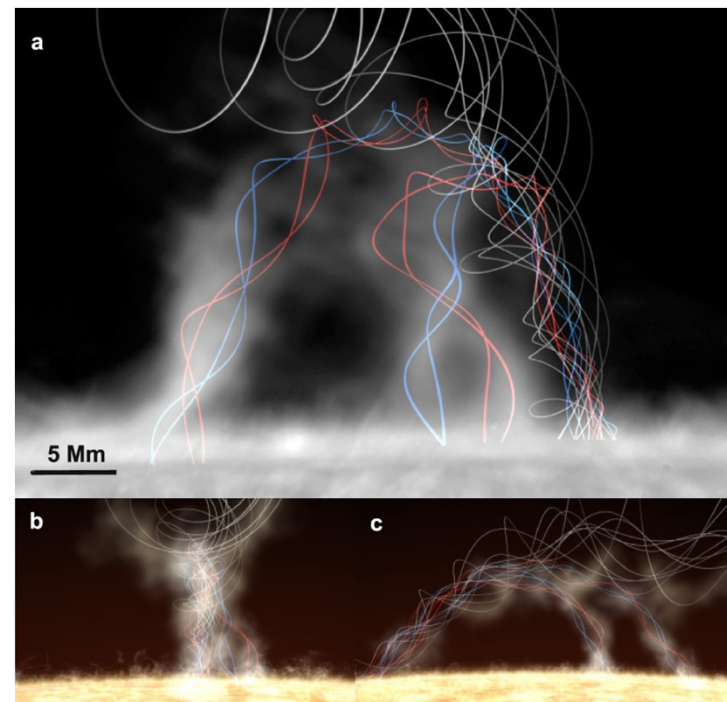
Depolarization alone also occurs if the magnetic field is oriented along the x axis (panel b): In this case the magnetic field mixes the radiatively excited circular oscillator states into the linear state aligned with the magnetic field. The more interesting special case is where the field is aligned along the LOS, i.e., along z (panel c). The observed light results from the circular states only.

SPECTRO-POLARIMETRIC IMAGING REVEALS HELICAL MAGNETIC FIELDS IN SOLAR PROMINENCE FEET

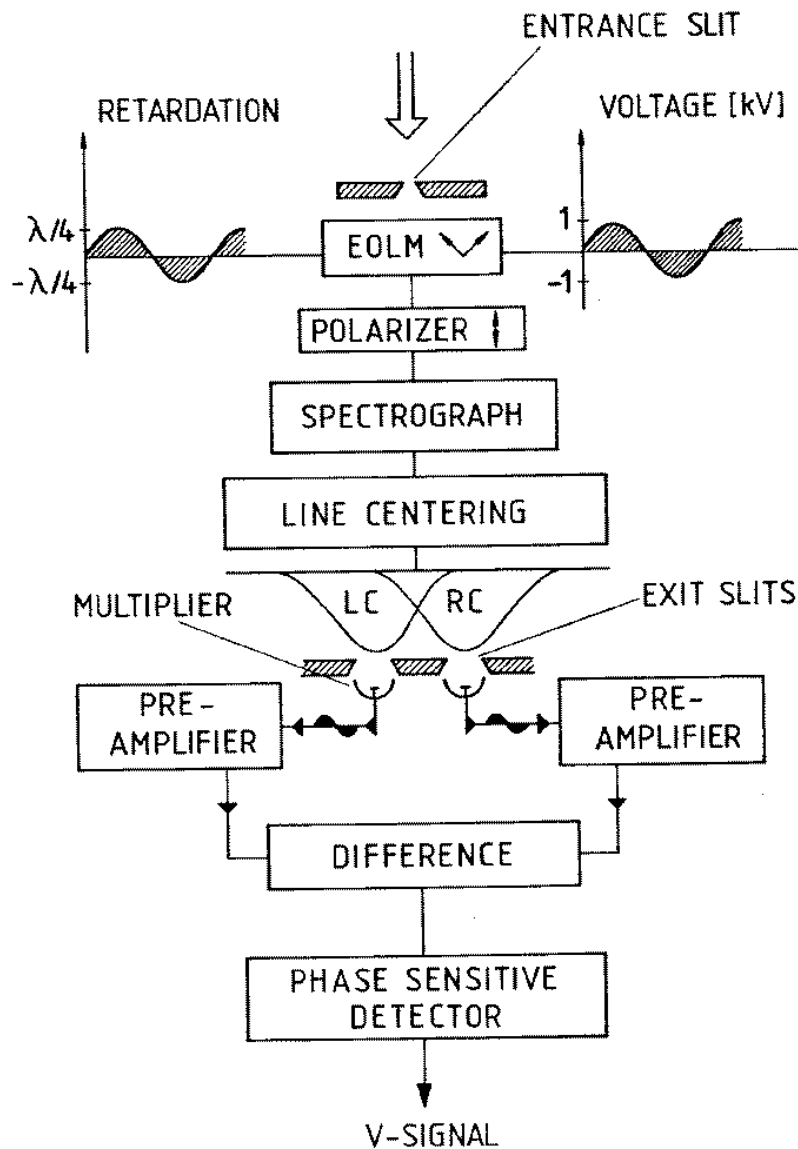
M. J. Martínez González et al, 2015, *Astrophys.J.*, 802:3.



Left images: (a) Inferred magnetic field topology of the prominence feet. Direction of the field projected onto the plane of the sky (short lines) overlaid to the intensity of the He I 1083.0 nm line and magnetic field strength (b). Short-dashed black lines in panel (a) trace the axes of the fibrils in the two feet. In the sketches below, blue arrows represent the actual inferred field vector in the f2a fibril. Note the opposite polarities of the magnetic field in both sides of the local vertical. This, and the relative inclination of the projected field with respect to the fibrils imply a helical field (red lines).



Magnetograph



This figure illustrates the principle of a photoelectric V -polarimeter. Behind the entrance slit is an electro-optic light modulator (EOLM): the orientation of the crystal and the applied AC voltage are chosen in such a way that the circularly polarized part of the light becomes linearly polarized.

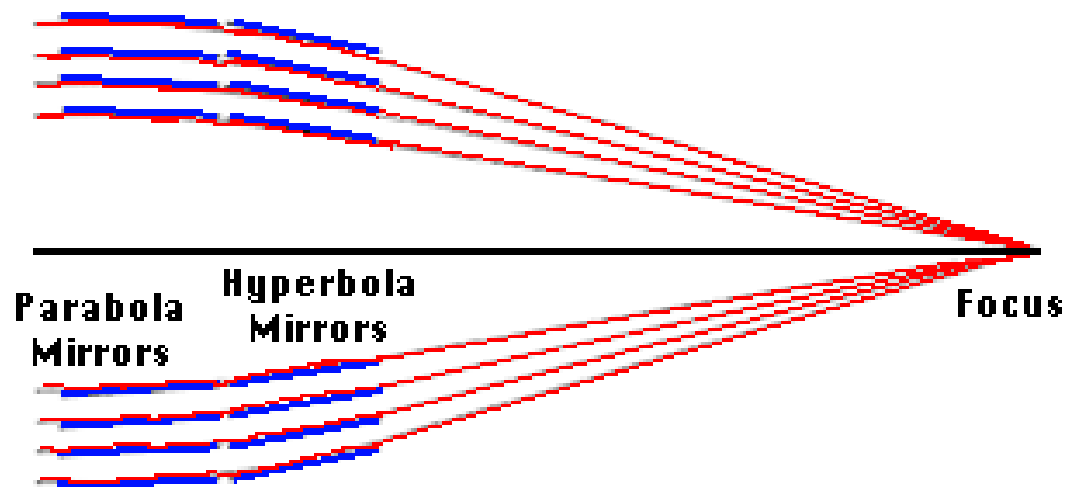
Thus, an intensity signal which alternately originates from the right and left circular polarization passes the polarizer and enters the spectrograph. A servo mechanism, e.g., the Doppler compensator, centers a magnetically sensitive line between two exit windows in the spectral plane.

An electronic device measures the difference between the two signals and, because of the modulation, recognizes the part which originally was circularly polarized. This part yields the desired V signal.

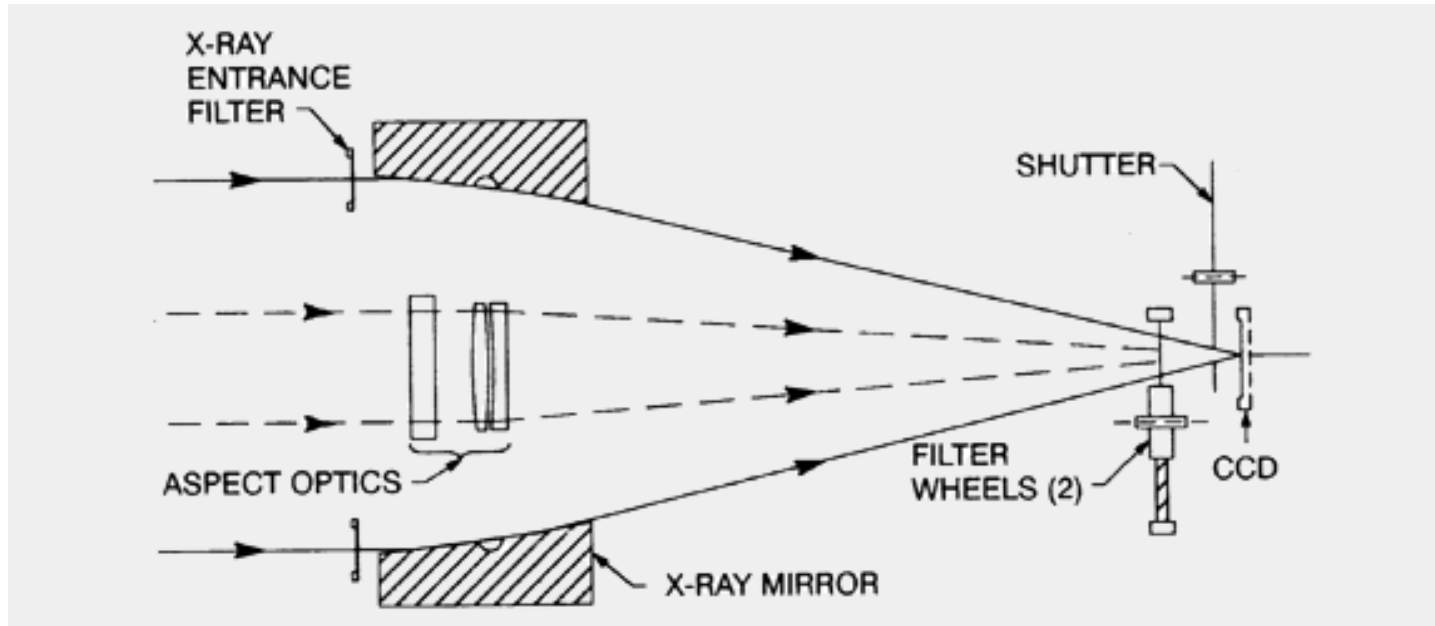
In solar physics a polarimeter is often called a *magnetograph* - the output signal is directly converted to a magnetic field strength by using the weak-field approximation.

X-ray Telescopes

The design of an X-ray imaging system is difficult because of the constraints imposed by the interaction of X-rays with matter. X-rays impinging at normal incidence (that is, perpendicular) on any material are largely absorbed rather than reflected. Normal incidence mirrors, like those used for optical telescopes, are thus ruled out. For an X-ray telescope, you must select a material which reflects the X-ray photon (so that the X-rays are not absorbed) and design your telescope so that the X-ray photons hit the mirror at small, so-called "grazing", incidence (so that they will be reflected). The most commonly used reflecting materials are gold and nickel for which the critical reflection angle at 1 keV is about 1 degree.



X-ray imaging system.



The SXT instrument on Yohkoh is a glancing incidence telescope of 1.54 m focal length which forms X-ray images in the 0.25 to 4.0 keV range on a 1024x1024 virtual phase CCD detector. A selection of thin metallic filters located near the focal plane provides the capability to separate the different X-ray energies for plasma temperature diagnostics. Knowledge of the location of X-ray images with respect to features observable in visible light is provided by a coaxially mounted visible-light telescope which forms its image on the CCD detector when the thin metallic filter is replaced by an appropriate glass filter.

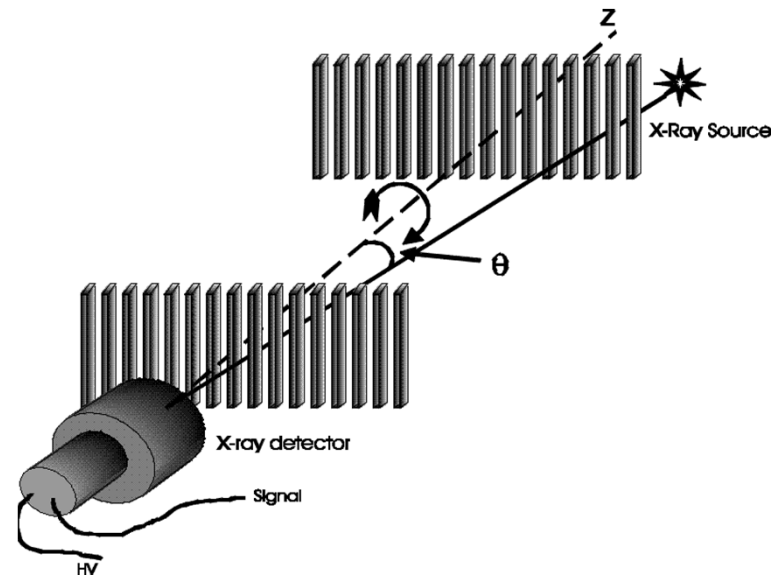
The RHESSI Mission.

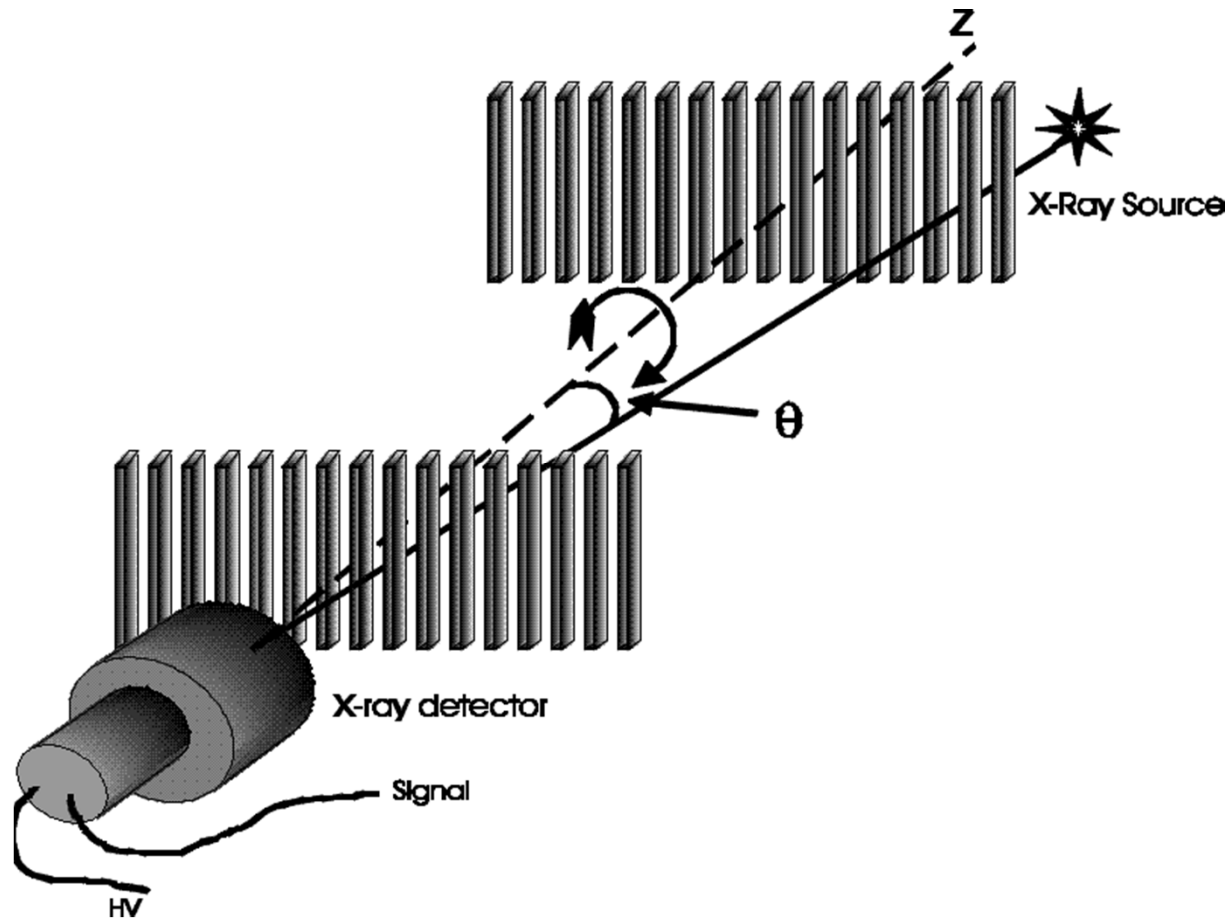
The RHESSI (Ramaty High Energy Solar Spectroscopic Imager) mission consists of a single spin-stabilized spacecraft in a 600km orbit inclined at 38° to the Earth's equator.

The only instrument on board is an imaging spectrometer with the ability to obtain high fidelity movies of solar flares in X-rays and γ -rays.

It uses two new complementary technologies: fine grids to modulate the solar radiation, and germanium detectors to measure the energy of each photon very precisely.

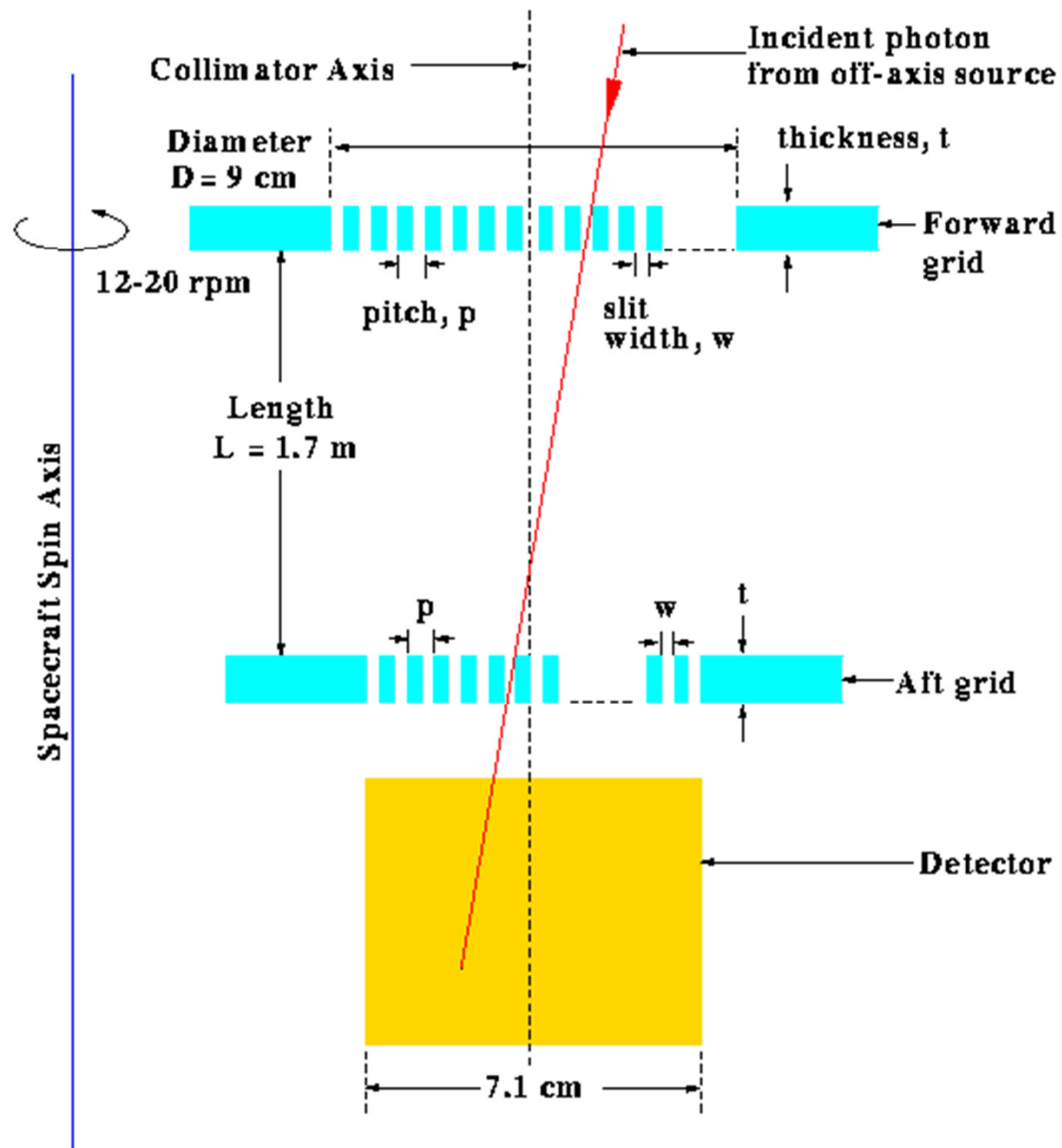
RHESSI's full Sun imaging capability is achieved with grids that modulate the solar X-ray flux as the spacecraft rotates at 15 rpm; up to 20 images can be obtained per second. The high-resolution spectroscopy uses germanium crystals that detect the X-ray and γ -ray photons transmitted through the grids over the broad energy range from 3 keV to 17 MeV.



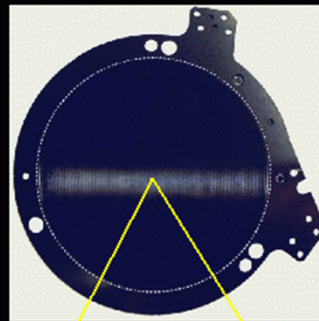


The grid pairs are coaligned so that they modulate the X-rays from a source that is off center from the axis of symmetry (labeled Z). The entire spacecraft is rotated so that the metal bars called slats block the source and then the openings called slits allow the source to shine on the detector. This means that the detector sees a brightening and darkening source in a regular pattern. The rate of change in the brightness is dependent upon the angle from the Z axis and the orientation of the source in the sky with respect to the rotating grid position.

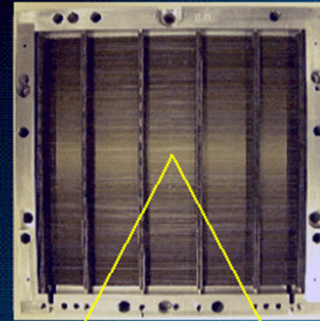
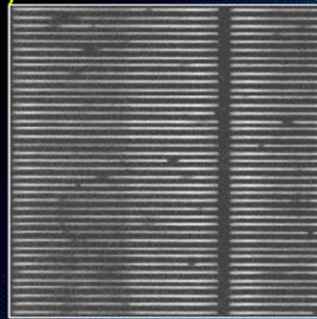
RHESSI grid parameters.



FLIGHT GRIDS #1 AND #5



Molybdenum / TECOMET
34 micron pitch, 1.25 mm thick
90 mm diameter



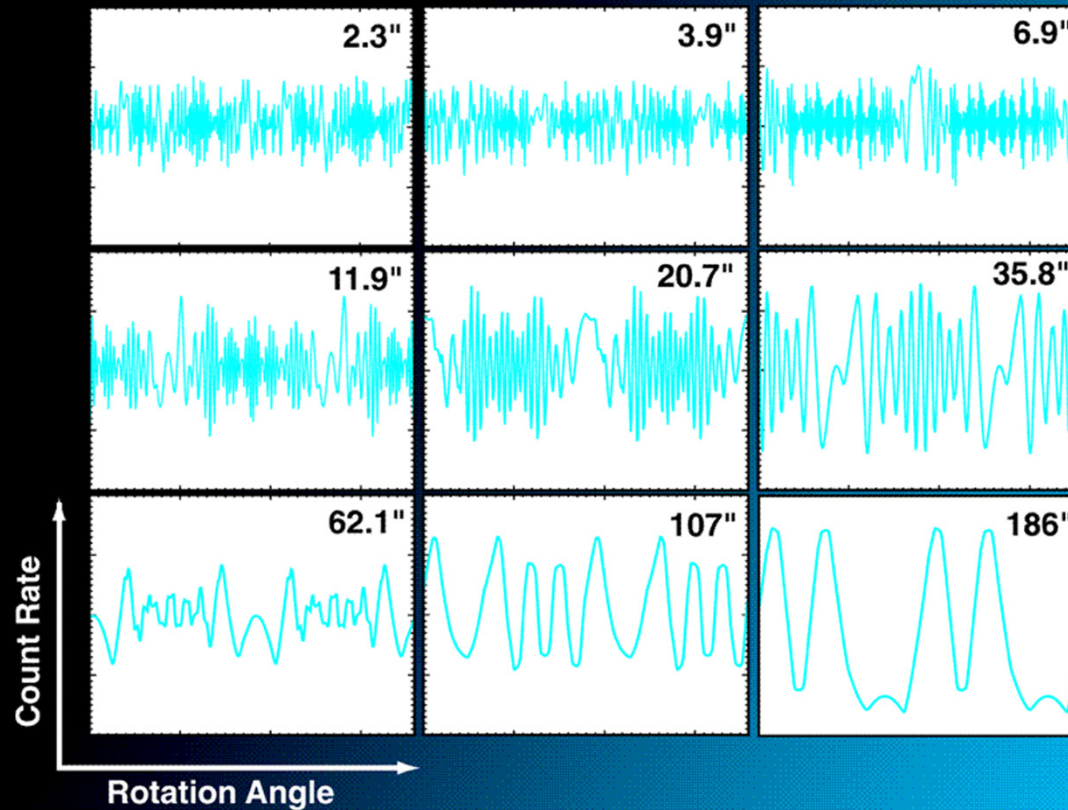
Tungsten / VBC
306 micron pitch, 10.7 mm thick
11 cm. X 11 cm.



Enlarged X-Ray Images taken at the
X-Ray Facility/GSFC

Nine grids are mounted on a grid tray at each end of the telescope tube. The grid pairs modulate the transmission of solar flare x-ray and gamma-ray emissions through to the detectors as the spacecraft spins around the axis of the telescope tube. The modulated count rates in the nine detectors are used in computers on the ground to construct images of solar flares in different energy bands.

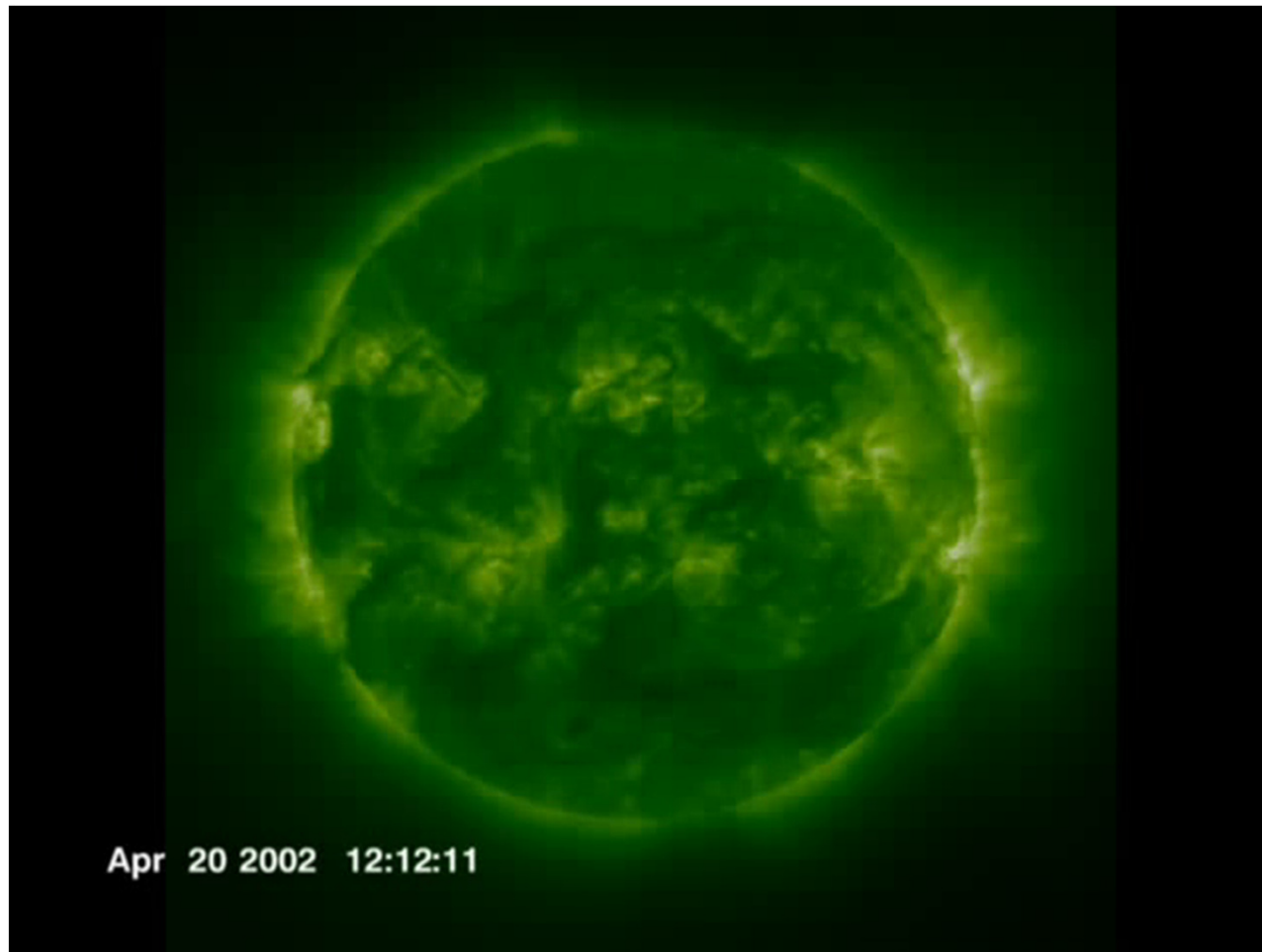
Count Rates in Each Detector for One Rotation

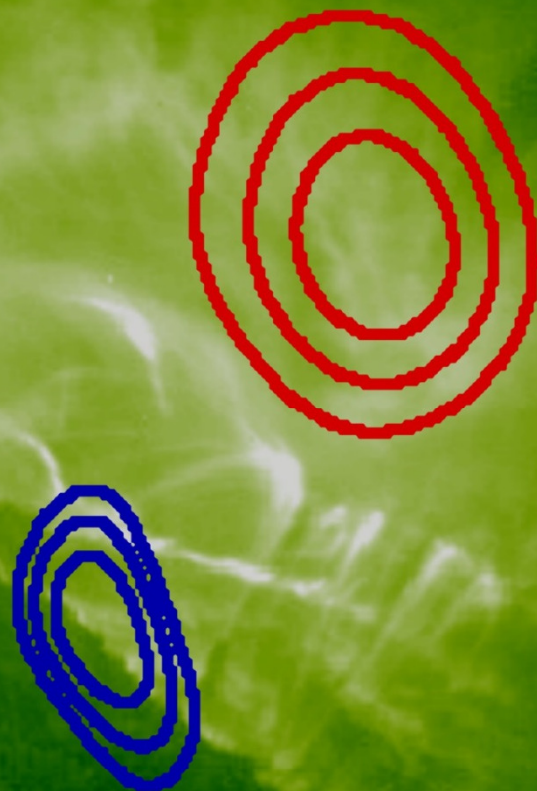


RHESSI count rates for various source positions. Image reconstruction techniques are used to obtain X-ray images from these counts.

RHESSI observations of X-rays sources of a solar flare

Zoom in (with rotation) to solar active region AR9906 on April 21, 2002 with SOHO/EIT,TRACE and RHESSI data. RHESSI observes x-rays from this flare. The red contours represent the 12-25 keV photon energy range and the blue contours represent 50-100 keV.





Apr 21 2002 01:31:08